



Separation and Determination of Zirconium from Environmental Water Samples Using Extractant Impregnated Resin

Dipak J. Garole^{1,2*}, Sandesh R. Tetgure¹, Bharat C. Choudhary¹, Pramod P. Patil¹, Amulrao U. Borse^{1*}, Surendra Prasad^{3*}

¹Department of Chemical Sciences, North Maharashtra University, Jalgaon 425001, Maharashtra, India ²Department of Geology and Mining, Government of Maharashtra, Nagpur 440010, India; ³Department of Biological and Chemical Sciences, School of Agriculture, Geography, Environment, Ocean and Natural Sciences, The University of the South Pacific, Suva, Fiji

ABSTRACT

In the present study, a novel and rapid extraction method using Extractant Impregnated Resin (EIR) prepared by impregnating Amberlite XAD-4 resin with Isonitroso-4-Methyl-2-Pentanone (IMP) was evaluated for separation and spectrophotometric determination of Zr⁴⁺ with arsenazo III at 670 nm. The optimization of various parameters influencing the sorption of Zr⁴⁺ in column and batch methods was carried. Zr⁴⁺ was quantitatively sorbed at pH 3.5 and recovered 99.2 ± 0.6% using 10 mL of 0.1 M oxalic acid as eluent in column method. The pre-concentration factor 200 with breakthrough volume 2000 mL and reusability up to 90 cycles were achieved with EIR. Experimental data were evaluated using the kinetic and isotherm models to explain the sorption mechanism of Zr⁴⁺ by EIR. The sorption equilibrium and kinetic data were best fitted in Dubinin-Radushkevich isotherm and pseudo second order, respectively. The mean energy (E_{DR}) of 11.47 kJ/mol for the sorption process suggested chemisorption of Zr⁴⁺ by EIR. The application of the developed method was assessed for Zr⁴⁺ extraction and determination in synthetic mixtures, tap, well and seawater samples. Overall, the experimental results of EIR strongly supported its potential as a future adsorbent for the extraction and determination of zirconium from water samples.

Keywords: Zirconium; Solid phase extraction; Extractant impregnated resin; Sorption; Pre-concentration

INTRODUCTION

Zirconium (Zr) is one of the important elements because of its use in the field of ceramic and nuclear industries, dental materials, surgical appliances, explosive primers, filaments, etc. [1-3]. It has been used extensively in water moderated reactors due to its inherent properties like low neutron absorption cross-section, excellent corrosion resistance at moderately elevated temperatures, strength, ductility, and ease of fabrication [4]. In addition, it is an ideal material for nuclear power stations as it does not absorb neutrons [5,6]. Considering these potential uses of Zr, its determination and recovery are extremely important from an environmental perspective. However, direct determination of Zr is still challenging and the problem becomes more strengthened due to limitations of instrumental techniques

and interference effects [7]. As a result, its selective separation and pre-concentration prior to analysis has been an important technique [8]. Various pre-concentration methods like solvent extraction [9,10], ion-exchange [11,12], ion imprinting polymers [13,14] and cloud point extraction [15,16] have been developed for its trace-level analysis. Liquid-liquid separation of Zr and hafnium from nitric liquor has also been used in order to obtain nuclear grade zirconium oxide using Tributyl Phosphate (TBP) as extractant [17]. Solvent extraction techniques using Methyl Isobutyl Ketone (MIBK) and TBP have also been extensively used in industrial separation and recovery of Zr [18,19]. However, these organic solvents have inherent limitations like solvents loss due to evaporation, environmentally non-benign, high aqueous solubility that forms an emulsion, disposal of spent liquid waste, as well as increasing interest in the user

Correspondence to: Dipak J. Garole, Department of Chemical Sciences, North Maharashtra University, Jalgaon 425001, Maharashtra, India; E-mail: drdipakgarole@gmail.com

Received: 05-Aug-2023, Manuscript No. ACE-23-22474; **Editor assigned:** 07-Aug-2023, PreQC No. ACE-23-22474 (PQ); **Reviewed:** 21-Aug-2023, QC No. ACE-23-22474; **Revised:** 04-Mar-2024, Manuscript No. ACE-23-22474 (R); **Published:** 11-Mar-2024, DOI: 10.35248/2090-4568.24.14.332

Citation: Garole DJ, Tetgure SR, Choudhary BC, Patil PP, Borse AU, Prasad S (2024) Separation and Determination of Zirconium from Environmental Water Samples Using Extractant Impregnated Resin. J Adv Chem Eng. 14:332.

Copyright: © 2024 Garole DJ, et al. This is an open access article distributed under the terms of the creative commons attribution license, which permits unrestricted use, distribution, and reproduction in any medium, provided the original author and source are credited.

health has prompted us to develop an alternative eco-friendly and economical method for separation of the analyte Zr.

Solid Phase Extraction (SPE) method has been gaining attention of researchers as practical and environment friendly separation of many organic and inorganic analytes [20-22]. Few SPE based methods have also been developed for Zr separation from the aqueous media and its determination at trace and ultra-trace levels [23-29]. Therefore, there has been increased interest to develop different types of adsorbents having high affinity, rapid adsorption rate, reusability, and the maximum adsorption capacity for analytes including Zr [30,31]. SPE based methods, particularly the impregnated sorbents, offer combined advantageous features of both; liquid-liquid extraction and ion exchange resins [32]. The extractant impregnated sorbents are easy to prepare where polymeric matrix resins are impregnated with an extractant having strong affinity for the selective ions [33]. In our previous work, extractant impregnated sorbents have been found to be promising materials for pre-concentration and determination of rare earth elements like uranium and thorium as well as heavy metals like nickel [34-36]. These extractant impregnated sorbents possessed good mechanical stability, reusable up to 80 cycles, and were able to pre-concentrate ultra-trace level of analytes of interest. Thus, to improve further sensitivity and reusability, the extractant Isonitroso-4-Methyl-2-Pentanone (IMP) was impregnated on Amberlite XAD-4 resin, characterized, and systematically investigated to devise the optimum conditions for the separation of Zr^{4+} . Therefore, in continuation of our study, the present study reports a systematic investigation for the sorption behavior of Zr^{4+} by Extractant Impregnated Resin (EIR) using column and batch mode followed by its spectrophotometric determination in different samples.

MATERIALS AND METHODS

Materials and instrumentation

A stock solution of 1.0 mg/mL Zr^{4+} was prepared by dissolving an appropriate quantity of Zirconyl Nitrate Monohydrate ($ZrO(NO_3)_2 \cdot H_2O$) (AR grade) purchased from Loba Chemie in slightly acidified Double Distilled Water (DDW). The working solution containing 20 $\mu\text{g/mL}$ of Zr^{4+} was prepared by

appropriate dilution. Amberlite XAD-4 resin (20-60 mesh size, surface area 750 m^2/g) was purchased from Supelco, Sigma Aldrich and cleaned by single washing sequentially with methanol, DDW, 1 M HNO_3 , water, 1 M $NaOH$, and DDW (till pH comes to neutral) to remove impurities and dried well before use. Arsenazo III (AR grade) was obtained from SD fine chemicals (India) and prepared 0.1% aqueous solution for spectrophotometric determination of Zr^{4+} . HCl solution of pH 3.5 was used to precondition the column.

Systronics digital pH meter 335 with a combined glass electrode was used for pH measurements. A Shimadzu 2450 UV-visible spectrophotometer with a 1 cm quartz cell was used for spectrophotometric determination of Zr^{4+} . A glass column (150 mm length-10 mm internal diameter, J-Sil make, India) was used for column studies. An orbital shaker, model BTI 39, from Bio-Technics India was used for batch experiments.

Experimental

The EIR was prepared and characterized using our earlier reported method. Briefly, an equal amount of extractant isonitroso-4-methyl-2-pentanone (1g) and the treated Amberlite XAD-4 resin (1g) were mixed in 20 mL methanol as a diluent for 5 hrs using an orbital shaker. Thus obtained EIR was oven dried to remove excess diluent followed by washing with dilute HCl and DDW. Then EIR was subjected to batch adsorption-desorption cycles for Zr^{4+} . All sorption and desorption experiments for Zr^{4+} removal was performed in triplicate at 298 K.

Experimental for column method

The EIR 100 mg was packed in a glass column having glass wool as support. The column was preconditioned with 25 mL of pH 3.5 solution of HCl. This was followed by Zr^{4+} sorption by passing a 25 mL aqueous solution containing 20 μg Zr^{4+} at optimized pH (3.5) with an optimum flow rate of 2 mL/min. The sorbed Zr^{4+} was desorbed using 10 mL of 0.1 M oxalic acid at the flow rate of 0.2 mL/min. Then Zr^{4+} was analyzed spectrophotometrically with arsenazo III at 670 nm [37]. The optimum conditions for sorption of Zr^{4+} are summarized in Table 1.

Table 1: Optimum conditions for sorption of Zr^{4+} by EIR.

Parameters	Optimum conditions
Aqueous phase pH	3.5
Flow rate for sorption (mL/min)	2
Concentration of oxalic acid for desorption	0.1 M
Flow rate for desorption (mL/min)	0.2
Pre-concentration factor	200
Breakthrough volume (mL)	≥ 2000

Relative standard deviation (%)	≤ 0.6
Average recovery (%)	98.5
Reusability cycles	90

Experimental for batch method

Batch mode experiments were performed to get insights into the sorption behavior of Zr^{4+} by EIR. 100 mg of EIR was pre-conditioned with 25 mL of pH 3.5 solution of HCl in 125 mL stoppered glass bottles i.e., shaking vessels. This was followed by the sorption of 25 mL Zr^{4+} solutions at different concentrations in the range of 4 mg/L-800 mg/L on preconditioned EIR. The sorption process was performed by shaking glass bottles for 40 min at 150 rpm and then allowed to settle for 10 minutes. The EIR was separated from the aqueous phase using Whatman filter paper no. 42. After sorption, recovery of Zr^{4+} was achieved using 10 mL of 0.1 M oxalic acid while shaking for 30 min at 100 rpm. The concentrations of Zr^{4+} before and after sorption were determined by spectrophotometrically with arsenazo III at 670 nm [37]. The amount of Zr^{4+} adsorbed per unit weight of EIR, q_t (mg/g) at time t was calculated using equation (1) where C_0 and C_t are the initial and liquid-phase concentrations of Zr^{4+} (mg/L) at time t , respectively, V is the volume (L) of Zr^{4+} solution and m is the mass (g) of EIR.

$$q_t = (C_0 - C_t) V / m \quad (1)$$

RESULTS AND DISCUSSION

Plausible extraction mechanism

The schematic illustration of a plausible mechanistic pathway for the sorption-desorption of Zr^{4+} by EIR is shown in Figure 1. As Amberlite XAD-4 resin has hydrophobic nature, it attracts the hydrophobic tail of the extractant molecules, which results in impregnation of resin by extractant. Step I show conditioning of EIR at pH 3.5 with HCl solution. After conditioning, Zr^{4+} forms a complex with the hydrophilic head of the extractant and results in sorption of Zr^{4+} (step II). This sorption is then followed by desorption step III, in which eluting agent (10 mL 0.1 M oxalic acid) forms a stronger complex as zirconium oxalate and results in desorption of sorbed Zr^{4+} . Thereafter, washing EIR material is reused for additional further sorption-desorption cycles.

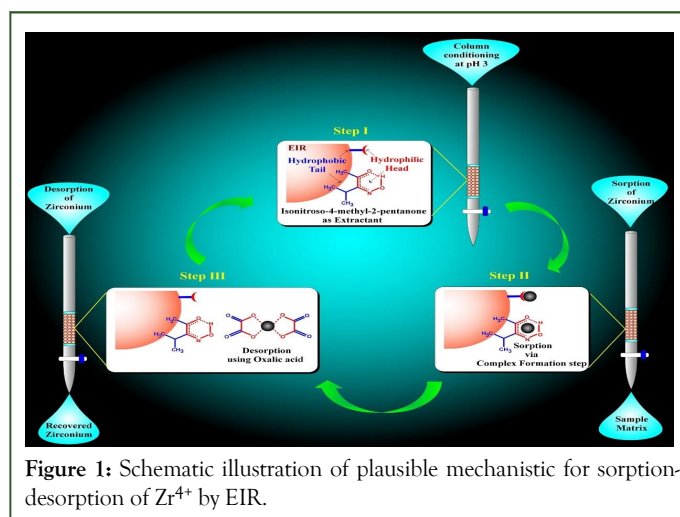


Figure 1: Schematic illustration of plausible mechanistic pathway for sorption-desorption of Zr^{4+} by EIR.

Column method

Optimization of pH

Sorption study of Zr^{4+} was found to be pH dependent. Therefore, sorption behavior from the analyte phase was studied in the pH range 1-6 using column mode under the experimental conditions: 25 mL aqueous solution containing $20 \mu g$ Zr^{4+} at the flow rate 2 mL/min and 10 mL eluent phase of 0.1 M oxalic acid at the flow rate 0.2 mL/min. The results of the pH dependence study are shown as a plot of percentage recovery against pH in Figure 2, which shows that initially the sorption increased with increasing pH 1 to 3. Then the highest sorption was quantitative between pH 3-4. Further increase in pH showed a drastic decrease in the sorption of Zr^{4+} up to pH 6. Therefore, pH 3.5 was considered as the optimum pH and used for further studies.

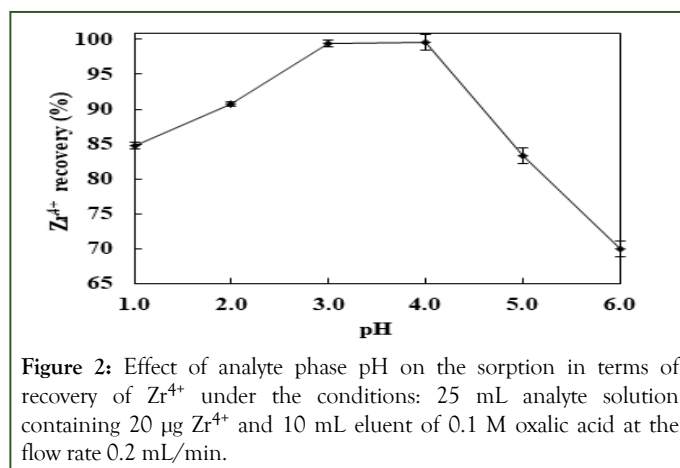


Figure 2: Effect of analyte phase pH on the sorption in terms of recovery of Zr^{4+} under the conditions: 25 mL analyte solution containing $20 \mu g$ Zr^{4+} and 10 mL eluent of 0.1 M oxalic acid at the flow rate 0.2 mL/min.

Effect of flow rate and volume

The frequency of analysis by column method in SPE depends on the flow rate of the analyte solution. Thus, the aqueous phase flow rate optimization was carried out by varying its flow rate from 0.5 to 3.5 mL/min. The result on the variation of flow rate is shown in the form of the plot of Zr^{4+} recovery against flow rate in Figure 3. It was observed that Zr^{4+} was quantitatively sorbed from 0.5 mL/min to 2.5 mL/min flow rate. On increasing the flow rates beyond 2.5 mL/min indicated a drastic decrease in the sorption of Zr^{4+} . Hence, the sample flow rate of 2 mL/min was considered optimum for further studies.

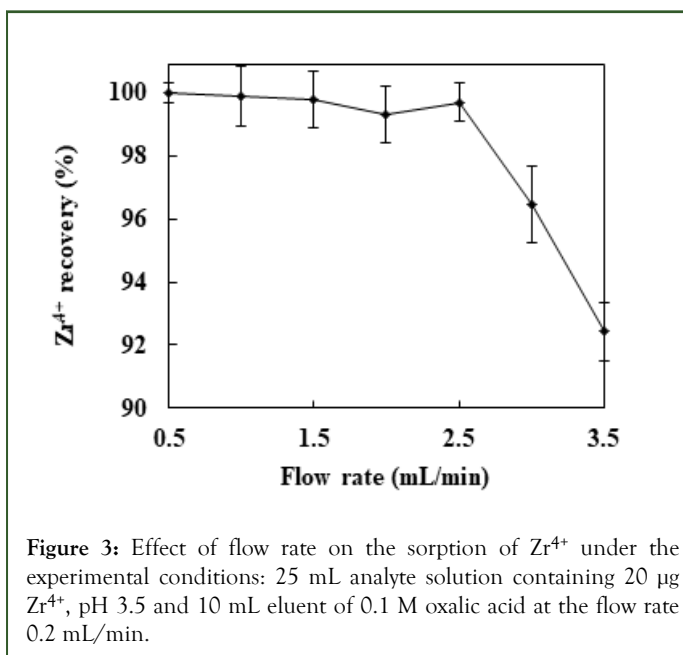


Figure 3: Effect of flow rate on the sorption of Zr^{4+} under the experimental conditions: 25 mL analyte solution containing 20 μ g Zr^{4+} , pH 3.5 and 10 mL eluent of 0.1 M oxalic acid at the flow rate 0.2 mL/min.

The Pre-concentration Factor (PF) is the major parameter for defining the superiority of a SPE method. It is given by the ratio of the maximum volume (mL) from which the analyte can be quantitatively recovered to the volume of eluent (mL) used for desorption of the analyte Zr^{4+} . Therefore, to optimize PF, different volumes of the analyte solutions (10 mL to 2000 mL) containing 20 μ g Zr^{4+} , were passed through the column at pH 3.5. The results in terms of the plot of Zr^{4+} recovery against sample volume is presented in Figure 4. The recovery of Zr^{4+} was found to be quite quantitative ($99.2 \pm 0.6\%$) up to 2000 mL of analyte solution.

Therefore, the optimum PF for the method was found to be 200, where the eluent volume used was 10 mL.

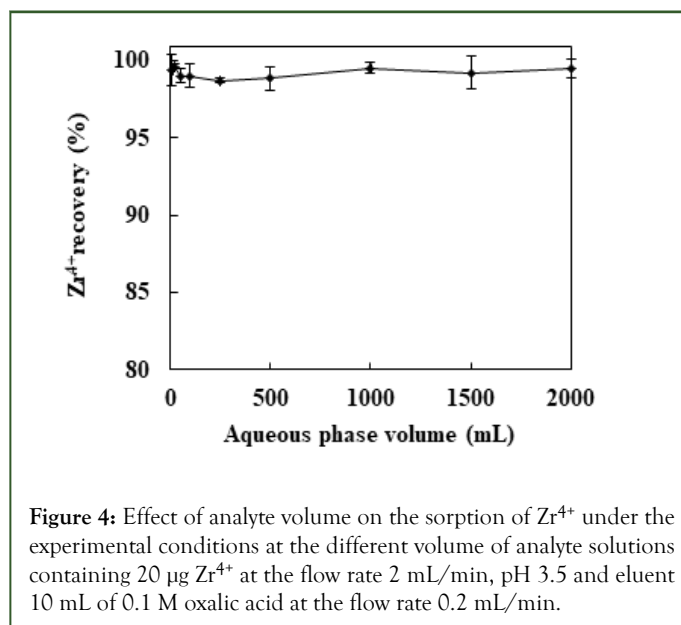


Figure 4: Effect of analyte volume on the sorption of Zr^{4+} under the experimental conditions at the different volume of analyte solutions containing 20 μ g Zr^{4+} at the flow rate 2 mL/min, pH 3.5 and eluent 10 mL of 0.1 M oxalic acid at the flow rate 0.2 mL/min.

Optimization of eluent phase parameters

The optimization of the eluent phase was carried out using different acids such as HCl, HNO_3 , H_2SO_4 , $HClO_4$, CH_3COOH , and oxalic acid ($H_2C_2O_4$) with their varied concentration from 0.01–4 M where recovery of Zr^{4+} was performed as its sorption. Table 2 summarizes the results due to different eluent with different parameters studied for recovery of Zr^{4+} using EIR in column mode. Table 2 clearly shows that the quantitative recoveries of $99.1 \pm 0.3\%$ and $99.2 \pm 0.6\%$ were achieved using 10 mL of 2 M H_2SO_4 and 0.1 M $H_2C_2O_4$, respectively, at the flow rate of 0.2 mL/min. However, the higher concentration of H_2SO_4 resulted in leaching, i.e., removal of extractant solvent from resin, and ultimately showed the diverse effect on reusability of EIR. Therefore, 10 mL of 0.1 M $H_2C_2O_4$ at the flow rate of 0.2 mL/min was used as an optimum eluent for further study. The recovery of Zr^{4+} using $H_2C_2O_4$ was possible due to formation of zirconium oxalate complex during desorption step III, as shown in plausible mechanism.

Table 2: Summary of eluent phase study using different acids with their varied concentrations.

Concentration ^a [M]	Recovery \pm RSD (%)					
	HCl	HNO_3	H_2SO_4	$HClO_4$	CH_3COOH	$H_2C_2O_4$
0.01	0.3 \pm 173.2	2.1 \pm 28.1	38.9 \pm 1.0	1.0 \pm 34.6	0.6 \pm 132.4	67.4 \pm 0.7
0.1	3.7 \pm 16.7	9.9 \pm 4.8	64.6 \pm 0.9	2.5 \pm 25.0	4.8 \pm 7.3	99.2 \pm 0.6
0.5	10.7 \pm 2.9	36.8 \pm 0.9	77.5 \pm 1.1	1.4 \pm 24.6	13.3 \pm 6.2	96.9 \pm 0.4
1	27.1 \pm 0.7	47.0 \pm 0.8	90.9 \pm 0.3	1.0 \pm 13.6	29.3 \pm 2.1	93.9 \pm 0.9
1.5	24.8 \pm 1.5	32.9 \pm 1.6	94.1 \pm 0.9	0.5 \pm 69.6	23.3 \pm 2.1	90.4 \pm 0.8
2	18.7 \pm 1.5	24.7 \pm 1.7	99.1 \pm 0.3	0.8 \pm 132.3	14.7 \pm 2.4	87.0 \pm 0.4

3	11.9 ± 1.1	17.1 ± 1.7	98.8 ± 0.3	0.4 ± 115.0	10.2 ± 10.6	82.0 ± 0.8
4	0.8 ± 114.5	6.6 ± 11.2	99.8 ± 0.3	0.4 ± 114.3	7.8 ± 7.3	76.8 ± 0.7
Eluent: 0.1M H₂C₂O₄						
Flow rate^b (mL/min)	Recovery ± RSD %	Volume^c (mL)	Recovery ± RSD (%)	Recovery ± RSD (%)		
0.2	99.2 ± 0.6	5	88.2 ± 0.8	88.2 ± 0.8		
0.4	96.6 ± 0.5	10	99.2 ± 0.6	99.2 ± 0.6		
0.6	94.7 ± 0.6	15	99.2 ± 0.5	99.2 ± 0.5		
0.8	90.1 ± 0.9					
1	86.5 ± 0.4					

Note: ^a10 mL different eluents with different concentrations (M) were used at flow rate 0.2 mL/min.

^b10 mL of 0.1 M H₂C₂O₄ was used at different flow rates.

^cDifferent volumes (mL) of 0.1 M H₂C₂O₄ were used at the flow rate 0.2 mL/min.

Stability test of column

The stability study of EIR was essential to establish the number of cycles for which the same EIR material could be used for successive and quantitative sorption and desorption process. The stability of EIR was calculated by passing a 25 mL sample solution containing 20 µg Zr⁴⁺ through the column, and the analyte Zr⁴⁺ was recovered with 10 mL of 0.1 M H₂C₂O₄, the results are presented in Figure 5. It was observed the column was relatively stable up to 90 cycles with 97.0 ± 0.9% recovery of Zr⁴⁺, which confirmed very high reusability and consistency of the developed EIR (Figure 5).

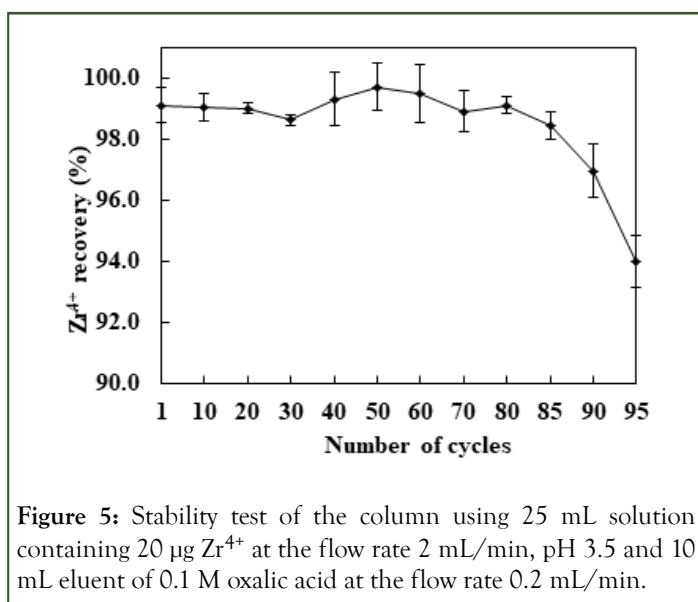


Figure 5: Stability test of the column using 25 mL solution containing 20 µg Zr⁴⁺ at the flow rate 2 mL/min, pH 3.5 and 10 mL eluent of 0.1 M oxalic acid at the flow rate 0.2 mL/min.

Effect of foreign ions

In general, real samples comprise of a matrix which can interfere in the analysis of the analyte. Therefore, setting up limits of interference for most commonly co-existing ions is one of the important parameters in developing SPE method. A known amounts of co-existing ions were added to 25 mL of the aqueous solution containing 20 µg of Zr⁴⁺ and recovery experiments were carried out using the developed column method. The tolerance limit was set as the maximum concentration of the foreign ions, which caused an approximately ± 2% relative error in the quantitative recovery of Zr⁴⁺. The results obtained shown in Table 3 show that the alkali and alkaline earth metal ions like.

Na⁺, K⁺, Ca²⁺ and Mg²⁺ had the highest tolerance limit up to 5000 µg. Some p-and d-block cations (Pb²⁺, Mn²⁺, Zn²⁺, Cd²⁺, V⁵⁺, Cr³⁺, Cr⁶⁺, Ni²⁺, Co²⁺, Al³⁺, Cu²⁺) had good tolerance limit in the range 1500 µg-400 µg. The anions of inorganic and organic acids have resulted in a good tolerance limit in the range of 5000 µg-100 µg. Rare-earth element interference was also studied, and many of them had low tolerance limits in the range of 300 µg-20 µg. Th⁴⁺, V⁴⁺, and Fe³⁺ had shown serious interference in Zr⁴⁺ sorption at 20 µg.

Table 3: Interference study of some common co-existing ions in the sorption of Zr^{4+} by EIRa.

Foreign ion	Tolerance limit (μg)	Foreign ion	Tolerance limit (μg)	Foreign ion	Tolerance limit (μg)
Cations		Rare earths		Anions	
Na^+ , K^+ , Ca^{2+} , Mg^{2+}	5000	Nd^{3+}	300	EDTA, NO_3^-	5000
Cd^{2+}	1500	Dy^{3+} , Ce^{4+} , Pr^{3+} , Sm^{3+}	150	SO_4^{2-} , PO_4^{3-}	3000
Pb^{2+} , V^{5+}	1000	La^{3+} , Gd^{3+} , Y^{3+}	100	Cl^-	1000
Zn^{2+} , Mn^{2+} , Cr^{3+}	750	Sc^{3+}	50	Oxalate	300
Sr^{2+}	600	U^{6+}	50	ClO_4^-	200
Cr^{6+} , Ni^{2+} , Co^{2+} , Al^{3+} , Ca^{2+} , Ba^{2+}	500	Th^{4+}	20 ^b	Tartarate, Citrate, CH_3COO^-	150
Cu^{2+} , Mg^{2+}	400			SCN^-	100
V^{4+} and Fe^{3+}	Interfere at 20 μg				

Note: ^aAqueous phase as 25 mL solution containing 20 μg Zr^{4+} at the flow rate 2 mL/min, pH 3.5 and eluent 10 mL of 0.1 M oxalic acid at the flow rate 0.2 mL/min.

^b Th^{4+} was masked with 1 mL 0.01 M EDTA.

Batch method

Evaluation of batch parameters

The first parameters evaluated in the batch method were shaking time and shaking speeds which are concerned with the environmental utility of SPE method developed for the sorptive removal of Zr^{4+} by EIR. The effect of shaking time was investigated from 5-120 minutes while shaking speed was in the range 50-200 rpm for Zr^{4+} sorption, i.e., extraction at pH 3.5 with initial Zr^{4+} concentration of 0.8 $\mu\text{g}/\text{mL}$ (i.e., 20 μg in 25 mL). The investigation results on shaking time and shaking speed optimization for Zr^{4+} sorption on EIR are shown in Figure 6. Initially, the sorption increased with contact time as well as shaking speed. It was observed that at 50 and 100 rpm shaking speeds, the sorption equilibrium time was 100 and 80 minutes, respectively and decreased as the shaking speed was increased. Figure 6 clearly shows that at the shaking speed of 150 and 200 rpm, equilibrium time came down to 40 minutes. Therefore, a shaking speed of 150 rpm and a shaking time of 40 minutes were taken as optimized conditions for further batch study.

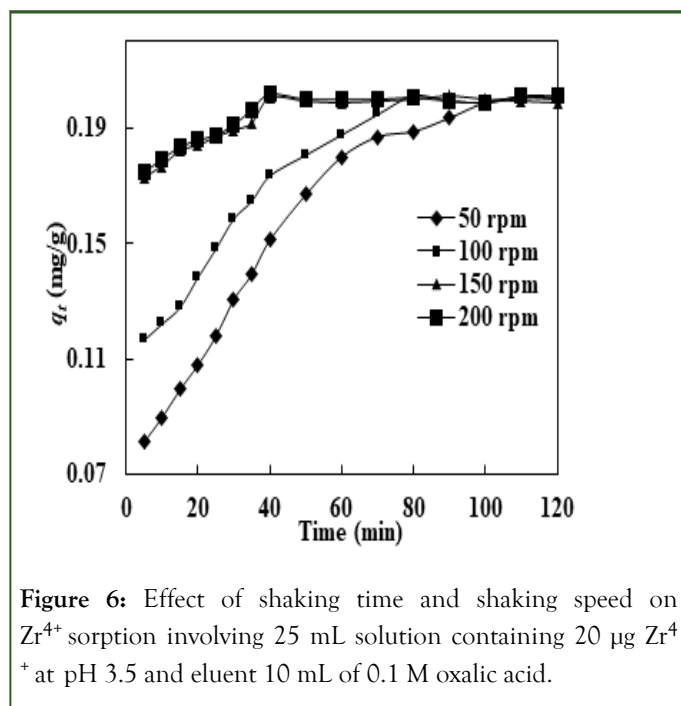


Figure 6: Effect of shaking time and shaking speed on Zr^{4+} sorption involving 25 mL solution containing 20 μg Zr^{4+} at pH 3.5 and eluent 10 mL of 0.1 M oxalic acid.

Kinetic behavior

The kinetic models like pseudo-first order, pseudo-second order, and the Weber-Morris pore diffusion [38] were used to explain the sorption behaviour of Zr^{4+} by developed EIR. The pseudo-first order, pseudo-second order, and the Weber-Morris pore diffusion models used in this study are shown in equations (2), (3), and (4), respectively where q_e , q_t , k_1 , k_2 , k_{id} and C are amount of sorbed solute at equilibrium condition ($mg\ g^{-1}$), the amount of sorbed solute ($mg\ g^{-1}$) at any time t (min), pseudo-first order rate constant (min^{-1}), pseudo-second order rate constant ($g\ mg^{-1}\ min^{-1}$), is the intraparticle diffusion model rate constant ($mg\ g^{-1}\ min^{-1/2}$), and intraparticle diffusion constant related to boundary layer thickness, respectively [39-41].

$$\log(q_e - q_t) = \log q_e - K_1 t / 2.303 \quad (2)$$

$$t/q_t = 1/K_2 q_e^2 + t/q_e \quad (3)$$

$$q_t = K_{id}(t^{1/2}) + C \quad (4)$$

The pseudo-first order and pseudo-second order rate equations (2) and (3), respectively, were used to explain the adsorption process of Zr^{4+} from the liquid phase [42]. The pseudo-first order plot of $\log(q_e - q_t)$ against time (t) is shown in Figure 7a showed the correlation co-efficient, $R^2=0.9936$. However, the pseudo-second order plot of (t/q_t) against time (t) (Figure 7b) was found to be strictly linear with a higher correlation coefficient ($R^2=0.9975$) than obtained in the case of pseudo-first order model. The values of q_e determined from pseudo-first order and pseudo-second order plots were found to be 0.0345 mg/g and 0.203 mg/g, respectively (Table 4). In addition, the q_e

(cal) value obtained from pseudo-second order equation was in agreement with the experimental value of q_e (0.201 mg/g). Therefore, the pseudo-first order model cannot describe the mechanism of Zr^{4+} sorption process developed by EIR. However, higher value of R^2 and quite close values of calculated and experimental q_e signpost the applicability of pseudo-second order kinetics to describe Zr^{4+} sorption process by developed EIR and confirmed that the adsorption process was surface reaction controlled with chemisorption involving valence forces through sharing or exchange of electrons between adsorbent and adsorbate (Figure 7) [43].

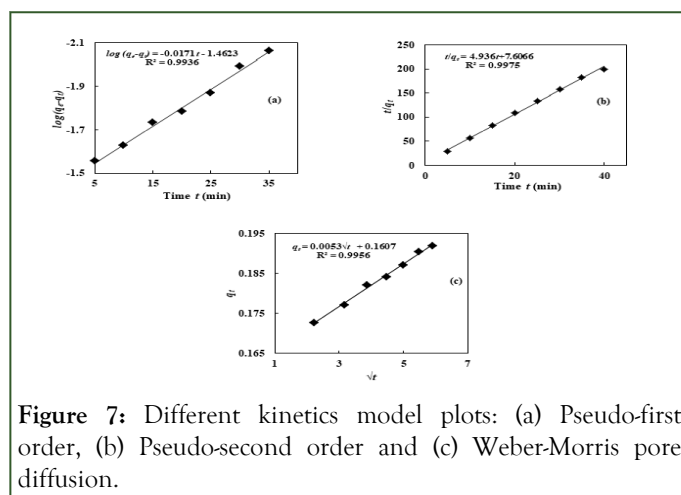


Figure 7: Different kinetics model plots: (a) Pseudo-first order, (b) Pseudo-second order and (c) Weber-Morris pore diffusion.

Table 4: Summarized results of kinetic behavior with respect to pseudo-second order, pseudo-second order and the Weber-Morris pore diffusion model.

Pseudo-first order	q_e ($mg\ g^{-1}$)	K_1 (min^{-1})	R^2
		0.0345	0.039
Pseudo-second order	q_e ($mg\ g^{-1}$)	K_2 ($g\ mg^{-1}\ min^{-1}$)	R^2
	0.203	3.203	0.9975
Weber-Morris pore diffusion	K_{id} ($mg\ g^{-1}\ min^{-1/2}$)	C	R^2
	0.0053	0.1607	0.9956

The diffusion of the sorbate into the interior pores of the resin bed is a generally slow process. The existence of such pore diffusion and determination of whether this pore diffusion is the rate determining step in the adsorption process was confirmed by the Weber-Morris pore diffusion or internal diffusion model [44]. A straight line with an intercept on the y-axis was observed in the Weber-Morris plot (Figure 7c), which suggested that rapid Zr^{4+} sorption by EIR was governed by both surface diffusion and pore diffusion process. The correlation coefficient ($R^2=0.9956$) and intercept ($C=0.1607$; Table 4) obtained from the Weber-Morris plot confirmed two different rate of mass transfer in the initial and final stages of sorption.

This also indicated some degree of boundary layer control, which implied that intra-particle diffusion was not only the rate-controlling step.

Isotherm behavior

The adsorption isotherms for Zr^{4+} sorption by EIR were obtained with different concentrations in the range of 4-800 mg/L at 298 K. The experimental results obtained are shown in Figure 8a in terms of plot of sorption capacity (q_e) against the concentration of Zr^{4+} . From the sorption capacity curve for Zr^{4+} sorption by EIR, q_e (exp) value was obtained as 24.28 mg/g. The linear form of Langmuir, Freundlich, and Dubinin-

Radushkevich (D-R) isotherm models shown in equations (5),(6), and (7), respectively, were applied to correlate the experimental data [45]. In these models, C_e , q_e , q_m , q_s , K_F , K_{DR} , b , n , E_{DR} and ϵ are solute aqueous concentration at equilibrium (mg/L), amount of solute sorbed per unit weight of sorbent at equilibrium (mg/g), Langmuir isotherm constant related to sorption capacity (mg/g), Dubinin-Radushkevich isotherm constant related to sorption capacity (mg/g), Freundlich isotherm constant related to sorption capacity ((mg/g)/(mg/L) n), Dubinin-Radushkevich constant related to the mean free energy of sorption (mol^2/kJ^2), Langmuir constant related to energy or net enthalpy of sorption (L/mg), Freundlich isotherm constant related to sorption intensity of the sorbent, mean energy of sorption process, and Dubinin-Radushkevich isotherm constant related to Polanyi potential calculated by equation ($\epsilon = RT \ln(1+1/C_e)$) at temperature (T in K) using the gas constant ($R=0.00813\text{kJ/mol K}^{-1}$), respectively (Table 5).

$$C_e/q_e = C_e/q_m + 1/q_m b \quad (5)$$

$$\log q_e = 1/n \log C_e + \log K_F \quad (6)$$

$$\ln q_e = \ln q_s - K_{DR} \epsilon^2 \quad (7)$$

$$E_{DR} = 1/(2K_{DR})^{1/2} \quad (8)$$

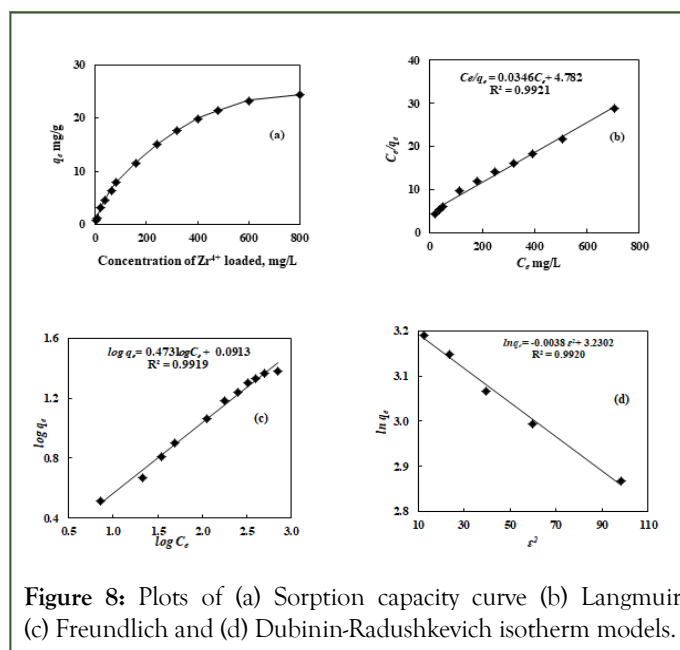


Figure 8: Plots of (a) Sorption capacity curve (b) Langmuir (c) Freundlich and (d) Dubinin-Radushkevich isotherm models.

Table 5: Isotherm parameters obtained from Langmuir, Freundlich and D-R models at 298 K.

Langmuir	q_m (mg/g)	b (L/mg)	R^2	
	28.9	0.0072	0.9921	
Freundlich	K_F (mg/g)	n	R^2	
	1.234	2.11	0.9919	
D-R	q_s (mg/g)	K_{DR} (mol^2/KJ^2)	E_{DR} (KJ/mol)	R^2
	25.27	0.0038	11.47	0.992

The calculated parameters for three different isotherm models have been shown in Table 5. Langmuir model assumes that a monolayer sorption occurs at energetically equivalent sites. The plot of C_e/q_e against C_e in Langmuir isotherm was found to be linear over the whole concentration range of 4-800 mg/L with correlation co-efficient, $R^2=0.9921$ (Figure 8b). Furthermore, values of q_m and b were calculated from the slope and intercept of the plot of Langmuir isotherm (Figure 8b) and were found to be 28.9 mg/g and 0.0072 L/mg (Table 5), respectively. Although the results could be well fitted and q_m value calculated; this is not the best model to be used for Zr^{4+} sorption with EIR. This is because the Langmuir model is applicable for homogeneous adsorbents, while EIR is a heterogeneous adsorbent, as has been characterized in the present study.

The applicability of the Freundlich isotherm model to the experimental data was important as this isotherm involves the sorption on a heterogeneous surface like EIR. This isotherm assumes that when the adsorbate concentration in the solution increases, its concentration on the adsorbent surface also increases. The Freundlich constants, K_F and n were calculated from the intercept and slope of the Freundlich isotherm plot of $\log q_e$ against $\log C_e$ (Figure 8c) and found to be 1.234 mg/g

and 2.11 mg/g, respectively (Table 5). The value of Freundlich constant (n) obtained was between 1 and 10 which confirmed a high sorption potential of EIR.

The D-R isotherm is based on the adsorption in micropores leading to pore-filling rather than layer by layer surface coverage, and it is applied to estimate the mean free energy of adsorption (ϵ), which is the energy required to transfer one mole of an adsorbate to the surface from infinity in solution. The value obtained for E_{DR} using the D-R plot of $\log q_e$ against ϵ^2 (Figure 8d) was 11.47 KJ/mol, which suggested that the sorption of Zr^{4+} by EIR involved a chemical sorption pathway. The sorption capacity q_s (cal) obtained from the D-R plot was found to be 25.27 mg/g (Table 5), which is in excellent agreement with q_e (exp.) (24.28 mg/g) obtained from the sorption capacity curve.

Analytical applications

Zr^{4+} determination from synthetic mixtures

The developed method was applied for the determination of Zr^{4+} at trace level in different synthetic mixtures (Table 6) as recovery of Zr^{4+} from 25 mL matrix. Table 6 shows that Zr^{4+} could be quantitatively determined from complex matrices. Th $^{4+}$

was co-extracted with Zr^{4+} , but its separation was achieved by masking Th^{4+} in an aqueous phase using 1 mL of 0.01 M EDTA.

Table 6: Determination of Zr^{4+} from some synthetic mixtures.

Composition of synthetic mixture (25 mL)	Recovery of Zr^{4+} (%) \pm RSD	
	Present method	ICP-OES method
Y^{3+} 10 μ g, V^{5+} 20 μ g, La^{3+} 40 μ g, Zr^{4+} 20 μ g	99.4 \pm 0.5	100.8 \pm 1.7
Ca^{2+} 30 μ g, Th^{4+} * 15 μ g, Cd^{2+} 30 μ g, Pb^{2+} 30 μ g, Zr^{4+} 20 μ g	99.2 \pm 0.3	101.4 \pm 6.1
Mg^{2+} 50 μ g, Y^{3+} 10 μ g, Th^{4+} * 10 μ g, Al^{3+} 30 μ g, Zr^{4+} 20 μ g	99.4 \pm 0.8	102.4 \pm 1.7

Note: * Th^{4+} was masked with 1 mL of 0.01 M EDTA.

Determination of Zr^{4+} from water samples

The developed column method was validated through checking recovery of Zr^{4+} from spiked water samples. All water samples were iso-kinetically collected in polyethylene bottles from different areas of Jalgaon and Mumbai (Maharashtra, India) and filtered through a membrane filter with a pore size of 0.45 μ m. Then 25 mL of each of the water of samples were spiked with

Table 7: Recovery of Zr^{4+} from different spiked water samples.

Samples (25 mL)	Zr^{4+} Added (μ g L ⁻¹)	Present method		ICP-OES	
		Found \pm SD (μ g L ⁻¹)	Recovery \pm RSD (%)	Found \pm SD (μ g L ⁻¹)	Recovery \pm RSD (%)
Tap water	0	BDL	BDL	BDL	BDL
	0.2	0.199 \pm 0.001	99.4 \pm 0.6	0.198 \pm 0.004	99.0 \pm 2.0
	0.4	0.400 \pm 0.002	100.0 \pm 0.5	0.398 \pm 0.0	99.5 \pm 0.0
Well water	0	BDL	BDL	BDL	BDL
	0.2	0.199 \pm 0.001	99.4 \pm 0.6	0.200 \pm 0.003	100.0 \pm 1.7
	0.4	0.400 \pm 0.002	100.0 \pm 0.5	0.393 \pm 0.012	98.4 \pm 3.0
Sea water	0	BDL	BDL	BDL	BDL
	0.2	0.199 \pm 0.001	99.4 \pm 0.3	0.199 \pm 0.001	99.7 \pm 0.5
	0.4	0.400 \pm 0.002	100.0 \pm 0.5	0.385 \pm 0.014	96.1 \pm 3.5

Note: BDL: Below Detection Limit.

CONCLUSION

The present study confirmed that the impregnation of Amberlite XAD-4 resin by extractant IMP is quite significant for the pre-concentration and determination of Zr^{4+} . Modification of resin resulted in the heterogeneous surface covered by extractant and was utilized for sorption of Zr^{4+} by chemisorption pathway. Sorption was quantitative at pH 3.5 with the flow rate of 2 mL/min and sorbed Zr^{4+} easily recovered 98.5 \pm 0.6% with 0.1 M oxalic acid (10 mL) at the flow rate 0.2 mL/min. The

different amounts of standard Zr^{4+} solution as shown in Table 7. The spiked samples were then subjected to the developed column method for the determination of Zr^{4+} and the recoveries of Zr^{4+} are reported in Table 7. The results show the quantitative recovery of Zr^{4+} in the range of 99.4%-100.0% from spiked water samples.

kinetics of the sorption process was well described using pseudo-second order model. The maximum sorption capacity of EIR for Zr^{4+} was calculated to be 25.27 mg/g using the D-R isotherm model. Based on the outcomes of the current work, the prepared EIR can be used as a promising adsorbent for the treatment of wastewaters containing Zr^{4+} upto 90 cycles.

ACKNOWLEDGEMENTS

Authors are thankful to the KBC North Maharashtra university for the laboratory facilities to carrying out the research. The author (S. Prasad) is grateful to the University of the South Pacific for support in various ways.

FUNDING

One of the authors (SRT) appreciates University Grant Commission (UGC), India, for the financial support given via the research fellowship in science for meritorious students (RFSMS) vide letter no. F.7-136/2007(BSR), dated 19/10/2012.

CONTRIBUTORS

All authors have contributed equally to this article.

CONFLICT OF INTEREST

The authors declare that they have no conflict of interest.

REFERENCES

- Afzali D, Fathirad F, Ghaseminezhad S, Afzali Z. Determination of trace amounts of zirconium in real samples after microwave digestion and ternary complex dispersive liquid-liquid microextraction. *Environ Monit Assess.* 2014;186:3523-3529.
- Bagda E, Tuzen M. Determination of zirconium in water, dental materials and artificial saliva after surfactant assisted dispersive ionic liquid based microextraction. *RSC Adv.* 2015;5:107872-107879.
- Ghasemi JB, Zolfonoun E. Simultaneous spectrophotometric determination of trace amounts of uranium, thorium, and zirconium using the partial least squares method after their pre-concentration by alpha-benzoin oxime modified Amberlite XAD-2000 resin. *Talanta.* 2010;80:1191-1197.
- Bassan MKT, Sharma PK, Singhal RK. Low cost and rapid analytical technique for determination of niobium and titanium in zirconium alloy. *Anal Methods.* 2010;2:1559-1564.
- Krishnan RMKA, Asundi MK. Zirconium alloys in nuclear technology. *Proc Indian Acad Sci Sect C: Eng Sci.* 1981;4:41-56.
- Suri AK. Material development for India's nuclear power programme. *Sadhana IASc.* 2013;38:859-895.
- Shokrollahi A, Gohari M. Flame atomic absorption determination of zirconium in glass and refractory bricks after coprecipitation with aluminium hydroxide. *J Taibah Univ Sci.* 2017;11:540-547.
- Srivastava B, Barman MK, Chatterjee M, Roy D, Mandal B. Solid phase extraction, separation and preconcentration of rare elements thorium (IV), uranium (VI), zirconium (IV), cerium (IV) and chromium (III) amid several other foreign ions with eriochrome black T anchored to 3-D networking silica gel. *J Chromatogr A.* 2016;1451:1-14.
- Pandey G, Mukhopadhyay S, Renjith AU, Joshi JM, Shenoy KT. Recovery of Hf and Zr from slurry waste of zirconium purification plant using solvent extraction. *Hydrometallurgy.* 2016; 163:61-68.
- Zhao J, Sui Y, Peng X, Sun G, Cui Y. A new diphosphonic acid extractant N, N-n-octylamine di(methylene phenylphosphinic acid) for extraction and separation of zirconium and hafnium in hydrochloric acid. *J Radioanal Nucl Chem.* 2020;324:339-348.
- Shvoeva OP, Dedkova VP, Savvin SB. Sorption-spectroscopy determination of zirconium on a PANV-KU-2 fibrous ion exchanger using arsenazo III. *J Anal Chem.* 2012;67:515-518.
- Smolik M, Jakobik-Kolon A, Poranski M. Separation of zirconium and hafnium using Diphonix® chelating ion-exchange resin. *Hydrometallurgy.* 2009;95:350-353.
- Chang X, Wang X, Jiang N, He Q, Zhai Y, Zhu X, et al. Silica gel surface-imprinted solid-phase extraction of Zr⁴⁺ from aqueous solutions. *Microchim Acta.* 2008;162:113-119.
- Sianipar A, Amran MB, Buchari B, Arcana IM. Effect of degree binary complex of imprint ion on the extraction of zirconium ion. *IOSR J Appl Chem.* 2012;1:15-19.
- Shariati S, Yamini Y. Cloud point extraction and simultaneous determination of zirconium and hafnium using ICP-OES. *J Colloid Interface Sci.* 2006;298:419-425.
- Ghasemi JB, Hashemi B, Shamsipur M. Simultaneous spectrophotometric determination of uranium and zirconium using cloud point extraction and multivariate methods. *J Iran Chem Soc.* 2012;9:257-262.
- Amaral JCBS, Souza AL, Morais CA. Liquid-liquid separation of zirconium and hafnium from nitric liquor in order to obtain nuclear zirconium oxide using TBP as extractant. *Chem Engg Comm.* 2020;207:73-83.
- Wang LY, Lee MS. A review on the aqueous chemistry of Zr(IV) and Hf(IV) and their separation by solvent extraction. *J Ind Eng Chem.* 2016;39:1-9.
- Xu L, Xiao Y, van Sandwijk A, Xu Q, Yang Y. Production of nuclear grade zirconium: A review. *J Nucl Mat.* 2015;466:21-28.
- Andrade-Eiroa A, Canle M, Leroy-Cancellieri V, Cerda V. Solid-phase extraction of organic compounds: A critical review. Part II. *Trends Anal Chem.* 2016;80:655-667.
- Ibrahim WA, Abd Ali LI, Sulaiman A, Sanagi MM, Aboul-Enein HY. Application of solid-phase extraction for trace elements in environmental and biological samples: A review. *Crit Rev Anal Chem.* 2014;44:233-254.
- Gupta NK, Choudhary BC, Gupta A, Achary SN, Sengupta A. Graphene based adsorbents for the separation of f-metals from waste solutions: A review. *J Mol Liquids.* 2019;289:21-23.
- Karve M, Gholave JV. Amberlite XAD-2 impregnated with Cyanex272 for zirconium(IV) enrichment followed by spectrophotometric determination. *Desalin. Water Treat.* 2014;52:1-3.
- Faghihian H, Kabiri-Tadi M. A novel solid-phase extraction method for separation and preconcentration of zirconium. *Microchim Acta.* 2010;168:147-152.
- Amin AS. Novel approach for the determination of zirconium by solid-phase spectrophotometry. *J Taibah Univ Sci.* 2015;9:227-236.
- Bhatti HN, Amin M. Removal of zirconium(IV) from aqueous solution by coriulus versicolor: Equilibrium and thermodynamic study. *Ecol Eng.* 2013;51:178-180.
- Dedkova VP, Shvoeva OP, Savvin SB. Sequential determination of nickel(II) and zirconium(IV) with dimethylglyoxime and arsenazo III after adsorption on one substrate disc. *J Anal Chem.* 2014;69:1037-1040.
- Zhang W, Ye G, Chen J. TRPO Impregnated leventrel resin: Synthesis and extraction behavior of Zr(IV) and Nd(III) ions. *Sep Sci Technol.* 2012;48:263-271.
- Yavari R, Davarkhah R. Application of modified multiwall carbon nanotubes as a sorbent for zirconium(IV) adsorption from aqueous solution. *J Radioanal Nucl Chem.* 2013;298:835-845.
- Wu H, Kim SY, Miwa M, Matsuyama S. Synergistic adsorption behavior of a silica based adsorbent toward palladium, molybdenum,

- and zirconium from simulated high level liquid waste. *J Hazard Mater.* 2021;411:125136.
31. Suneesh AS, Selvan BR, Prathibha T, Sriram S, Ramanathan N. Extraction chromatography based separation of zirconium(IV) from simulated high level liquid waste using N,N-di-octyl-2-hydroxyacetamide impregnated amberlite XAD-7 resin. *CE J Advances.* 2021;8:100182.
 32. Chakraborty R, Asthana A, Singh AK, Bhawana J. Adsorption of heavy metal ions by various low-cost adsorbents: A review, *Inter J Env Anal Chem.* 2022;102:342-379.
 33. Kabay N, Cortina JL, Trochimczuk A, Streat M. Solvent-Impregnated Resins (SIRs)-methods of preparation and their applications. *React Funct Polym.* 2010;70:484-496.
 34. Tetgure SR, Garole DJ, Borse AU, Sawant AD. Novel extractant impregnated resin for thorium pre-concentration from different environmental samples-column and batch study. *Sep Sci Technol.* 2015;50:2496-2508.
 35. Tetgure SR, Choudhary BC, Garole DJ, Borse AU, Sawant AD, Prasad S. Novel extractant impregnated resin for pre-concentration and determination of uranium from environmental samples. *Microchem J.* 2017;130:442-451.
 36. Tetgure SR, Choudhary BC, Borse AU, Garole DJ. Column and batch sorption investigations of nickel(II) on extractant-impregnated resin. *Env Sci Pollu Res.* 2019;26:27291-27304.
 37. Snell FD. Photometric and fluorometric methods of analysis of metals, John Wiley and Sons, New York. 1978.
 38. Faghihian H, Kabiri-Tadi M. Removal of zirconium from aqueous solution by modified clinoptilolite. *J Hazard Mater.* 2010;178: 66-73.
 39. Choudhary B, Paul D. Isotherms, kinetics and thermodynamics of hexavalent chromium removal using biochar. *J Env Chem Eng.* 2018; 6: 2335-2343.
 40. Garole DJ, Choudhary BC, Paul D, Borse AU. Sorption and recovery of platinum from simulated spent catalyst solution and refinery wastewater using chemically modified biomass as a novel sorbent. *Env Sci Poll Res.* 2018;25:10911-10925.
 41. Tran HN, You SJ, Hosseini-Bandegharai A, Chao HP. Mistakes and inconsistencies regarding adsorption of contaminants from aqueous solutions: A critical review. *Water Research.* 2017;120:88-116.
 42. Qiu H, Lv L, BC Pan, Zhang QJ, Zhang WM, Zhang QX. Critical review in adsorption kinetic models. *J Zhejiang Univ Sci.* 2009;10:716-724.
 43. Nayak NB, Nayak BB. Aqueous sodium borohydride induced thermally stable porous zirconium oxide for quick removal of lead ions. *Sci Rep.* 2016;6:23175:1-12.
 44. Weber WJ, Morris JC. Kinetics of adsorption on carbon from solution. *J Sanitary Eng Division ASCE.* 1963;89:31-60.
 45. Xu Y, Kim SY, Usuda S, Wei Y, Ishii K. Adsorption and desorption behavior of tetravalent zirconium onto a silica based macroporous TODGA adsorbent in HNO₃ solution. *J Radioanal Nucl Chem.* 2013;297:91-96.